ELSEVIER

Journal of Nuclear Materials 290–293 (2001) 1–11

journal of nuclear materials

www.elsevier.nl/locate/jnucmat

Section 1. Reviews

Plasma–wall interaction issues in ITER

G. Janeschitz *, ITER JCT and HTs

ITER Joint Central Team, ITER–JWS–Garching, Boltzmanstrasse. 2, 85748 Garching, Germany

Abstract

In 1998 the four ITER parties decided to investigate a smaller and cheaper (50% cost) machine design with reduced technical objective but without jeopardizing the programmatic objective. Based on various design studies a machine with 6.2 m major radius and aspect ratio 3.1 has been selected. Two main regimes of operation are foreseen namely ELMy H-mode and steady-state operation, the latter in discharges with internal transport barriers (ITB). In ELMy H-mode, an important issue is the maximum tolerable energy for repetitive pulsed energy loads (ELMs) of 0.4 and 0.64 MJ m^{-2} for CFC and W, respectively, in order to achieve adequate divertor lifetimes (ca. a few 1000 discharges). Based on present predictions there is only a marginal compatibility of the expected ELM energy loads with these thresholds. Reducing the ELM size, by gas puffing, tends to reduce also the energy confinement. The regimes with ITB may pose a problem for the divertor operation due to the expected low plasma edge density and the large power crossing the separatrix (up to 130 MW). Using the present knowledge about plasma–wall interaction (erosion in steady and pulsed loads, re-deposition as well as of tritium co-deposition), the majority of the plasma facing surface has to be clad with Be and W. At present, a small area of CFC at the divertor strike zones is foreseen in the reference design. However, due to the relatively high T co-deposition rate predicted, the use of CFC may not be possible in a D–T machine. © 2001 Elsevier Science B.V. All rights reserved.

Keywords: ITER; Divertor; Plasma–wall interaction; Next-step device

1. Introduction

In this paper we will discuss plasma–wall interaction issues in the "Next Step" machine ITER. Already in earlier studies of possible next step machines [1–6] it became clear that plasma–wall interaction issues are among the most important problems to be solved along the way towards a fusion reactor. It was understood early on that new divertor physics solutions [3,7] are required to achieve consistency between divertor engineering possibilities and the expected divertor plasma parameters and peak power loads in a machine like ITER. During the initial phase of the EDA it became also clear that there is a threshold for acceptable ELM energy losses due to surface evaporation of the divertor targets [8] and that also disruptions (thermal quench, vertical displacement events (VDE)) and run away electrons (RAE) will have a major impact on the lifetime as well as on the design of the 'In Vessel' components [9]. In addition tritium trapping due to co-deposition and implantation, dust production most likely during disruptions [10], as well as plasma pollution due to impurities migrating from the PFCs into the main plasma complete the catalogue of plasma–wall interaction issues to be tackled by a combination of physics and engineering design.

Plasma–wall interaction issues, and in particular their magnitudes, are strongly related to the plasma performance as well as the operation modes of a particular machine. Therefore, a discussion of plasma–wall interaction issues is intimately coupled with a discussion of the general scope of a machine and of the planned operation scenarios as well as with the plasma-facing materials (PFM) choice. To this end a brief description of the objectives and of the parameters of the new ITER is given here. A more detailed discussion of the methodology to arrive at this parameters and of the performance in the various envisaged operation modes is given in [11].

* Tel.: +49-89 3299 4111; fax: +49-89 3299 4165.
E-mail address: janescg@itereu.de (G. Janeschitz).

PII: S0022-3115(00)00623-1

Due to the fact that the ITER parties felt unable to provide the necessary funds for constructing the 1998 ITER, it was decided to investigate the possibility of designing a machine with somewhat reduced technical objectives [12] and thus significantly reduced cost (the goal is to achieve 50% of the 1998 ITER cost). They new objectives are:

1. an energy amplification factor of 10, i.e. $Q = 10$, in inductive operation;
2. the goal to achieve $Q = 5$ in non inductive steady-state operation, i.e., with a pulse length in the order of >3000 s;
3. a minimum pulse length of >400 s in inductive operation,
4. an average neutron wall loading of >0.5 MW m^{-2}, and a total fluence of 0.3 MW m^{-2}.

The enhanced emphasis on steady-state is supported by the discovery of new regimes with internal transport barrier (ITB), during the last 5 years [13–17]. These ITB regimes display higher energy confinement than in H-mode and can in principle achieve relatively large bootstrap current fractions (up to 70%). They are now the basis for steady-state operation scenarios in a reduced size ITER and all options studied were as much as possible optimised also for these regimes.

In addition to improved physics knowledge [11,18] gives rise to changes in some of the physics (design) rules specified in [19]. The two most important changes are:

1. present experiments show that high pedestal pressures (high pedestal temperatures) and thus high triangularity is required to achieve good energy confinement in H-mode at densities near the Greenwald limit [20–25];
2. to achieve acceptable divertor target power loads (<10 MW m^{-2}) and sufficient neutral pressure for He exhaust at the expected power flow into the scrape-off layer (SOL) (75–130 MW) a divertor volume accommodating for vertical targets and a minimum upstream separatrix density at the outer midplane (>3.0×10^{19} m^{-3}) are required [26–28].

Several machine layouts with different aspect ratio all having a capability to achieve a fusion performance of $Q = 10$ where investigated [11,29]. It was concluded that an intermediate aspect ratio machine (IAM; $A_I = 3.1$; Table 1) should be the basis of a new outline design for ITER [11]. This decision is mainly based on the higher operation density (+20%), when compared to a low aspect ratio machine, which provides more margin for a satisfactory divertor performance, and on the advantages for steady-state operation, i.e. the higher bootstrap current at a given β_N.

2. Plasma–wall interaction issues in relation to plasma edge and core physics

Two main operation modes are envisaged for ITER, namely the ELMy H-mode (Type-I ELMs) and the hybrid or steady-state operation with an ITB and large current drive power (up to 100 MW). Both modes of operation will cause specific plasma–wall interaction problems which are also related to the plasma facing materials used and/or to the engineering solutions adopted.

2.1. ELMy H-mode

During the last few years a basic understanding of the relation between the H-mode pedestal (temperature) and the core energy confinement has emerged [20–25,30–32]. As a result a minimum temperature at the top of the pedestal is required, namely the turning point temperature (TPT), i.e., the pedestal temperature at which the confinement behavior changes from 'stiff' to 'nonstiff' temperature profile behavior, is required in order to achieve good H-mode confinement (Fig. 1) [24]. With

Table 1
Main parameters of ITER–FEAT

Parameter	Unit	Nominal	Limits
Major radius, R	m	6.2	<=
Minor radius, a	m	2.0	<=
Plasma current, I_p	MA	15[a]	17[b]
Additional heating & CD power	MW	73	100
Fusion power	MW	500	700
Toroidal field at major radius, Bo	T	5.3	<=
Elongation at 95% flux, $\kappa_{95,}\kappa_X$		1.7, 1.85	<=
Triangularity at 95% flux, $\delta_{95,}\delta_X$		0.33, 0.49	<=
Plasma volume	m^3	837	<=
Plasma surface	m^2	678	<=
MHD safety factor at 95% flux, q_{95}		3	2.6
Average neutron wall load at the first wall	MW/m^2	0.57	0.80

[a] >400 s.
[b] ~100 s.

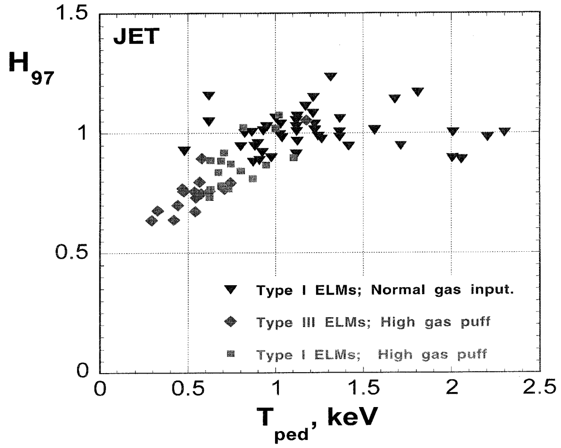

Fig. 1. The H-factor normalized to the H97 scaling versus the temperature on top of the pedestal (T_{ped}) for discharges with different gas puff scenarios and ELM types in JET. The H-factor in discharges with low pedestal temperature is proportional to T_{ped} (characteristic for stiff temperature profiles) while it becomes independent of T_{ped} at high pedestal temperatures (nonstiff branch).

increasing density the pedestal temperature decreases due to the fact that the pedestal width, the maximum pressure gradient in the pedestal (ballooning limited) and thus the pressure on top of the pedestal is at best more or less constant for a given set of parameters (I_P, triangularity, etc.). This results in a need for high pedestal pressures (high triangularity) and thus high pedestal energy content if one wants to operate with good confinement at high normalized density ($T_{Ped} > \mathrm{TPT}$). Due to the large pedestal energy content in these high triangularity Type-I ELM scenarios (high pedestal pressure) larger energy losses during ELMs can be expected and are in fact observed [20,33].

In order to evaluate the TPT for ITER, which can be seen as an optimized operation point, the simple analytical model presented in [24] is employed which yields a TPT in the order of 3.5 keV. This pedestal temperature is in the same range as the ones predicted to be required for good H-mode confinement by detailed transport code calculation based on ITG models, e.g., in [30].

The energy loss per ELM in ITER can be evaluated by using the above pedestal temperature (TPT $\sim$ 3.5 keV) and assuming 80% of the line average density (1.0×10^{20} m^{-3}) as pedestal density. This yields an energy stored in the pedestal of $\sim$107 MJ (53.5 MJ electron energy). In order to estimate the energy loss per ELM in ITER two approaches are possible. An empirical scaling based on ELM energy loss fractions in DIII-D and JET [33] which predicts that 31 $\pm$ 5% of the pedestal electron energy is lost during a Type-I ELM. In a more physical interpretation one can assume that the amount of ELM energy lost is determined by the ratio of two characteristic times; namely the transport time along fieldlines $\tau_{//}$, which is determined by the ion sound speed considering pedestal top plasma parameters in the SOL during an ELM, and the time of enhanced cross field transport τ_{ELM} in the pedestal and SOL during an ELM. In order to have a significant impact of $\tau_{//}$ one needs to assume also that $\tau_{\mathrm{ELM}} \ll \tau_{//}$. Based on this 'ansatz' the ELM energy loss fraction can be written as:

$$\frac{W_{\mathrm{ELM}}}{W_{\mathrm{ped}}} = \frac{1}{1 + \tau_{//}/\tau_{\mathrm{ELM}}} \frac{W^0_{\mathrm{ELM}}}{W_{\mathrm{ped}}},$$

where $W^0_{\mathrm{ELM}}/W_{\mathrm{ped}}$ is the energy fraction lost during an ELM if the transport in the SOL would be infinite. In order to determine the two unknowns in the above formula (i.e., $W^0_{\mathrm{ELM}}/W_{\mathrm{ped}}$ and τ_{ELM}) the ELM energy loss fraction as well as other relevant parameters of a low- and a high-density discharge from DIII-D were used. The such calibrated expression was then applied to discharges from several machines (DIII-D [34], DIII-D [35], JT60U, ASDEX-UP) and reasonably good agreement was found. However due to the limited amount of data used in this comparison it cannot be excluded that $W^0_{\mathrm{ELM}}/W_{\mathrm{ped}}$ and τ_{ELM} display also some dependencies, e.g., on plasma current and power flux, if this ansatz is compared to an extended data set.

However, regardless of such dependencies, as long as $\tau_{\mathrm{ELM}} \ll \tau_{//}$ a significant reduction of the ELM energy loss predicted for ITER can be expected from the above ansatz when compared to the empirical scaling. In ITER the characteristic transport time in the SOL is $\sim$310 μs and thus twice as long as the one in JET and JT60U. This results in a $\sim$50% lower pedestal energy loss fraction than the one observed in JET and JT60U when using the above physics ansatz.

In order to decide whether ELMs are tolerable for the divertor targets of ITER one has to be aware that during a 400 s discharge approximately 1000 ELMs will occur and that the lifetime of the targets should be in the order of several 1000 discharges. Due to the large number of ELMs during the life of an ITER divertor target evaporation and melt layer losses are unacceptable which will, however, occur if the power deposition limits [36] reported in Table 2 for CFC and W targets, respectively, are exceeded. From Table 2 one can see that an energy load of only 0.4 MJ m^{-2} and 0.64 MJ m^{-2} is allowed for CFC and W targets, respectively, when assuming an energy deposition time of 0.3 ms. The total allowed energy loss from the plasma during an ELM depends also on the surface area which receives this load (see Table 2). From present day machines we know that there is either no broadening of the strike zones (S_{SS} in Table 2) or at most a factor 2 widening of the main power deposition area [32]. Combining the energy deposition limits with the expected energy

Table 2
Allowable Energy deposition on the divertor targets during ELMs[a]

	C (0.3 ms)	W (0.3 ms)
Allowable energy deposition E (MJ/m^2) for 10^6 ELMs, deposition time = 0.3 ms	0.4	0.93 (0.64)
Allowable W_{ELM} (MJ) for 10^6 ELMs with deposition area $S = S_{SS} = 8$ m^2	3.2	7.44 (5.1)
Allowable W_{ELM} (MJ) for 10^6 ELMs with deposition area $S = 2 \times S_{SS} = 16$ m^2	6.4	14.9 (10.2)

[a] ( ): considering melting.

loss during ELMs in ITER (using the empirical as well as the physics based scaling of the ELM energy loss fraction) yields the results shown in Fig. 2 for CFC (Fig. 2(a)) and W targets (Fig. 2(b)). The variation of the energy loss per ELM over fusion power in Fig. 2 is obtained by using the proportionality between fusion power and stored energy.

From Fig. 2 it can be seen that the energy loss per ELM exceeds the allowable level for vaporisation/melting of the divertor plates in particular for CFC targets in most cases except for low fusion power when using the physics based extrapolation of the ELM energy loss. However, W targets could withstand standard Type-I ELMs for the physics based extrapolation of the ELM energy loss or if the energy loss extrapolated by the empirical ELM energy loss scaling can be reduced by ~ factor 2 (e.g., by gas puffing, etc.).

In many machines it has been demonstrated that the energy loss per ELM can be reduced by triggering ELMs externally (e.g., by pellets) or increasing the ELM frequency (by, e.g., gas puffing). However, this reduction of the ELM energy loss is in most cases realized by decreasing the pedestal temperature (and possibly pressure), which inevitably results in a decrease in the H-factor [34]. Beside the Type-I ELMy regime another H-mode regime with high pedestal pressure, good confinement and small or no ELMs exists. It is called either grassy ELM [37], Type-II ELM [38] or enhanced D-alpha (EDA) [39,40] regime and might be a backup solution for the reference Type-I ELM regime in ITER. However, based on present knowledge it can only be obtained at $q_{95\%} > 3.5$ and at high triangularity >0.4. Only if more data and a better understanding of this regime is available it will be possible to assess its applicability to an ITER like machine.

The RI mode is another possible high confinement regime and can in principle be understood in the same way as the pellet injection discharges from the high field side, i.e., the peaking of the density profile compensates the reduction of the pedestal pressure or in extreme cases the existence of an L-mode edge by directly improving the ITG caused transport [41]. The relevance of this operation regime for ITER must be demonstrated on large machines (e.g. JET, JT60U), before this scenario can be employed as a backup for the Type-I ELMy H-mode.

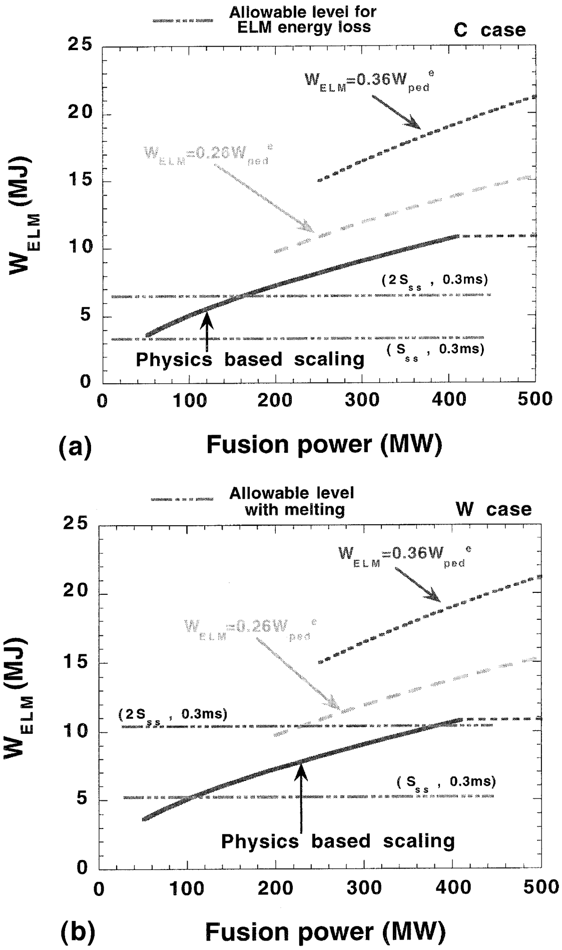

Fig. 2. (a) Predicted ELM energy loss range (W_{ELM}) for the empirical (dashed lines) and the physics based (solid line) scaling and the allowable pulsed energy load for a CFC target assuming no widening of the deposition area (S) and a factor 2 widening of the deposition area ($2S$). As one can see the predicted ELM energy loss exceeds the allowable above 200 MW fusion power even for the physics based scaling. (b) Predicted ELM energy loss range (W_{ELM}) for the empirical (dashed lines) and physics based (solid line) scaling and the allowable pulsed energy load for a W target (melt limits). As one can see the predicted ELM energy loss (physics based scaling) has some overlap with the limits defined by melting.

2.2. Steady-state scenarios with ITB

The second general type of discharges in ITER beside ELMy H-mode are those with an internal transport barrier (ITB) which may allow the achievement of $Q = 5$ in hybrid (long pulse) or steady-state operation [13–17,19]. Two general types can be distinguished, namely a regime with monotonic but low central shear (optimized shear regime – OSR) and a reversed shear regime (RSR). Additional features are peaked density profiles, relatively low line average density (low edge density) and relatively high plasma heating, i.e. in ITER, alpha particle heating of <100 MW and additional heating of up to 100 MW for current drive. Concerning plasma–wall interaction, the issues are the low edge and SOL densities, high power flux into the SOL (higher than in ELMy H-mode) as well as an improved core plasma confinement for He [42] and possibly for other impurities. Large ELMs seem not to be a problem in this kind of discharges because, due to the ITB, the importance of the H-mode pedestal pressure for energy confinement is reduced.

Modeling the ITER–SOL and divertor plasma with B2-EIRENE [28] shows that for power fluxes into the SOL in the order of 75 MW an upstream density (at the separatrix at the outer midplane) $\sim 3.0 \times 10^{19}$ m^{-3} is required to keep the peak power load at the outer divertor target below 10 MW m^{-2}. Recent modeling results [28] show that a V-like structure near the strike zone (enhancing neutral recycling) can reduce the peak power load on the targets significantly (by $\sim$30%) without a reduction in He exhaust efficiency. This allows either to operate at lower upstream density or at higher SOL power (up to 100 MW). In discharges where up to 130 MW of power flows into the SOL, which will most likely be the case for hybrid and steady-state scenarios, a V-like divertor geometry near the strike zone [28] will be required together with a relatively high upstream density ($>3.3 \times 10^{19}$ m^{-3}). Therefore, a modified divertor geometry as shown in Fig. 3 is presently studied from the engineering as well as from the physics point of view. Even with this optimized geometry it is questionable whether the peak power at the target can be kept below the engineering limit of 10 MW m^{-2} in hybrid or steady-state scenarios. Achievement of high SOL densities will be also difficult because the good properties of ITB discharges tend to disappear when strong gas puffing is applied [13–17]. A rule of thumb is that for good energy confinement in ITBs, as well as in H-mode, the ratio between line average density and upstream separatrix density should not be less than 3. While there are a few examples where this number is smaller in H-mode without strong confinement degradation, ITB discharges seem to be more sensitive to gas puffing or to an edge and SOL density increase.

The engineering limit of 10 MW m^{-2} could be raised in particular if the plasma-facing material is W [9] (the 2 cm thick CFC cladding would start to evaporate at >15 MW m^{-2}) and if the fatigue lifetime of the target heat sink (the CuCrZr tubes or hypervapertrons) turns out to be acceptable (results from ongoing R&D).

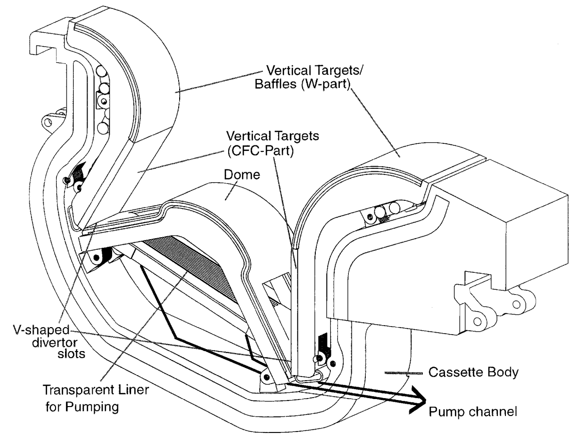

Fig. 3. A possible new divertor geometry presently under investigation which might allow to reduce the target power load by $\sim$30%.

The ability to pump He in discharges with higher than 10 MW m^{-2} peak power on the divertor target remains satisfactory as long as the He partial pressure in the divertor private region is not reduced significantly (sufficient upstream density for a high recycling divertor and thus low divertor plasma temperatures (<15 eV) near the strike zone). However, as already mentioned, the core He confinement seems to be significantly increased in ITB discharges [42], when compared to ELMy H-mode which makes He ash removal more difficult.

In conclusion the core plasma regimes have a significant impact on the PFC design and on the choice of PFM. Vice versa the choice of the PFC design and the choice of PFMs will in turn influence the performance of the envisaged core plasma regimes considerably and may well decide if certain regimes are feasible. Based on the present understanding of the interaction between the envisaged core plasma regimes and the divertor, W seems to have significant advantages over CFC as plasma facing material for the divertor strike zones. However, from the above considerations it becomes also clear that the compatibility of the required core performance and the ability to absorb the consequent heat fluxes (pulsed and steady-state) by a realistic PFC design with adequate lifetime is in many cases marginal (even with W).

3. Plasma facing component lifetime, T-co-deposition, and dust issues

This section discusses the expected erosion lifetime of the plasma facing components with emphasis on the divertor targets as well as related issues such as tritium co-deposition and dust produced from the various PFMs. Since erosion and T-co-deposition are discussed in detail in [6,36] they will be only treated briefly here.

3.1. Component lifetime

When assessing the erosion lieftimes of plasma facing components one has to distinguish between normal operation and abnormal events such as disruption thermal quenches and VDEs and define the percentage of discharges where these abnormal events occur (i.e., in 10% of the discharges). Considering normal operation and excluding the discussion of ELMs treated in the previous section, one can distinguish between the main chamber wall, where no re-deposition of the sputtered material will take place, and the divertor targets, where re-deposition and thus also T-co-deposition (mainly for CFC targets) will occur. In the case of abnormal events the divertor will receive large energy loads (up to $\sim$30 MJ m^{-2}) within less than 1 ms during disruption thermal quenches while the main chamber wall can experience also large energy loads (up to 60 MJ m^{-2}) during vertical displacement events (VDEs) lasting up to 300 ms as well as during run-away electron generated loads [43].

3.1.1. Main chamber wall

The candidate PFMs for the main chamber wall are Be [44] (Fig. 4(a)) and possibly W. Erosion in normal operation is caused by charge exchange (CX) neutrals and hydrogenic as well as impurity ions being intercepted by the wall before they reach the divertor. Eroded first wall (FW) material will be most likely ionized in the SOL and will be transported to the divertor with little chance ($\ll$10%) to reach the wall or the main plasma. Therefore, most of this material will be deposited in the divertor and can in principle contribute among other things to T-co-deposition.

An assessment of the lifetime of the FW clad with 1 cm thick Be and W, respectively, yield an erosion rate of several 10^{-2} nm s^{-1} for Be and approximately a factor 10 less for W [36] with a moderate peak near the gas puff in case of Be and less so for W (Fig. 4(b)). While the erosion of 0.3–1 cm per burn year in case of Be is certainly acceptable for a low duty factor machine like ITER, it is not acceptable for a power producing reactor. Therefore, a W clad wall will ultimately be required in a reactor (10 burn years lifetime based on erosion by sputtering only) providing a strong incentive to start investigations on the compatibility of high Z main chamber walls with the envisaged plasma regimes in ITER.

When considering abnormal events such as VDEs and run-away electrons the choice between W and Be is not so clear. A large number of analyses were performed on the impact of VDEs on the FW, both in terms of erosion and lifetime [9,43,45,46] as well as in terms of survival of the heat sink. In cases where a VDE with maximum power causes an energy deposition of $\sim$60 MJ m^{-2} for longer than 300 ms at the same location it is likely that the blanket cooling channels will burn out, melt and a water leak with all its consequences (long recovery time) will occur. In this case a 1 cm thick Be cladding protects the heat sink better due to its lower evaporation and melt temperatures than does a W cladding. Due to the movement of the plasma during VDEs and due to preceding thermal quenches in most cases, it is unlikely that such a severe energy load will occur. In addition the use of killer pellets can in principle be foreseen as a mitigation method [47]. However, it is not clear if killer pellets (e.g., Be) would not create run-away electrons and thus only transfer the problem to another area of the FW instead of solving it. A possibility for killer pellets which will not cause run-aways is the injection of a large amount of deuterium by a liquid deuterium jet, but no design for such a device exists to date.

The amount of melting and evaporation losses per VDE of a plasma that has not undergone a preceding thermal quench has been analyzed, with [43] and without [45,46] a vapor shield. Assuming that all melted and evaporated material will be lost in such cases yields erosion rates of $\sim$0.2–0.4 mm (with vapor shield) to $>$1.0 mm (without vapor shield) for a Be clad wall and 0.35–0.7 (with vapor shield to $>$1.0 mm (without vapor shield) for a W clad wall respectively for each VDE. From this result a W clad wall will suffer approximately twice the erosion per VDE than a Be clad wall in cases with vapor shield suggesting that for an experimental machine like ITER a Be FW seems to be the right choice while for a reactor where VDEs should in principle not occur a W wall will most likely be optimum.

3.1.2. High heat flux components

The PFMs envisaged for the divertor high heat flux (HHF) components are CFC and W (Fig. 4(a)). In the divertor, erosion of the targets by sputtering (including chemical sputtering in the case of CFC), as well as re-deposition of the eroded materials, occurs together with the deposition of material originating from the FW. Due to the complexity of these processes codes like REDEP [48] have to be applied using a plasma background solution produced by the B2-EIRENE code in order to obtain quantitative answers [36]. Summarizing the results, the erosion lifetime of the CFC divertor targets is in the order of 7000 discharges or 20 cm/burn year which is an improvement when compared to the 1998 ITER design and can be explained by the somewhat different plasma solutions found with B2-EIRENE for ITER. While this lifetime is certainly adequate for ITER it would be unacceptable for a reactor. The erosion due to sputtering, in case of W clad divertor targets, is negli-

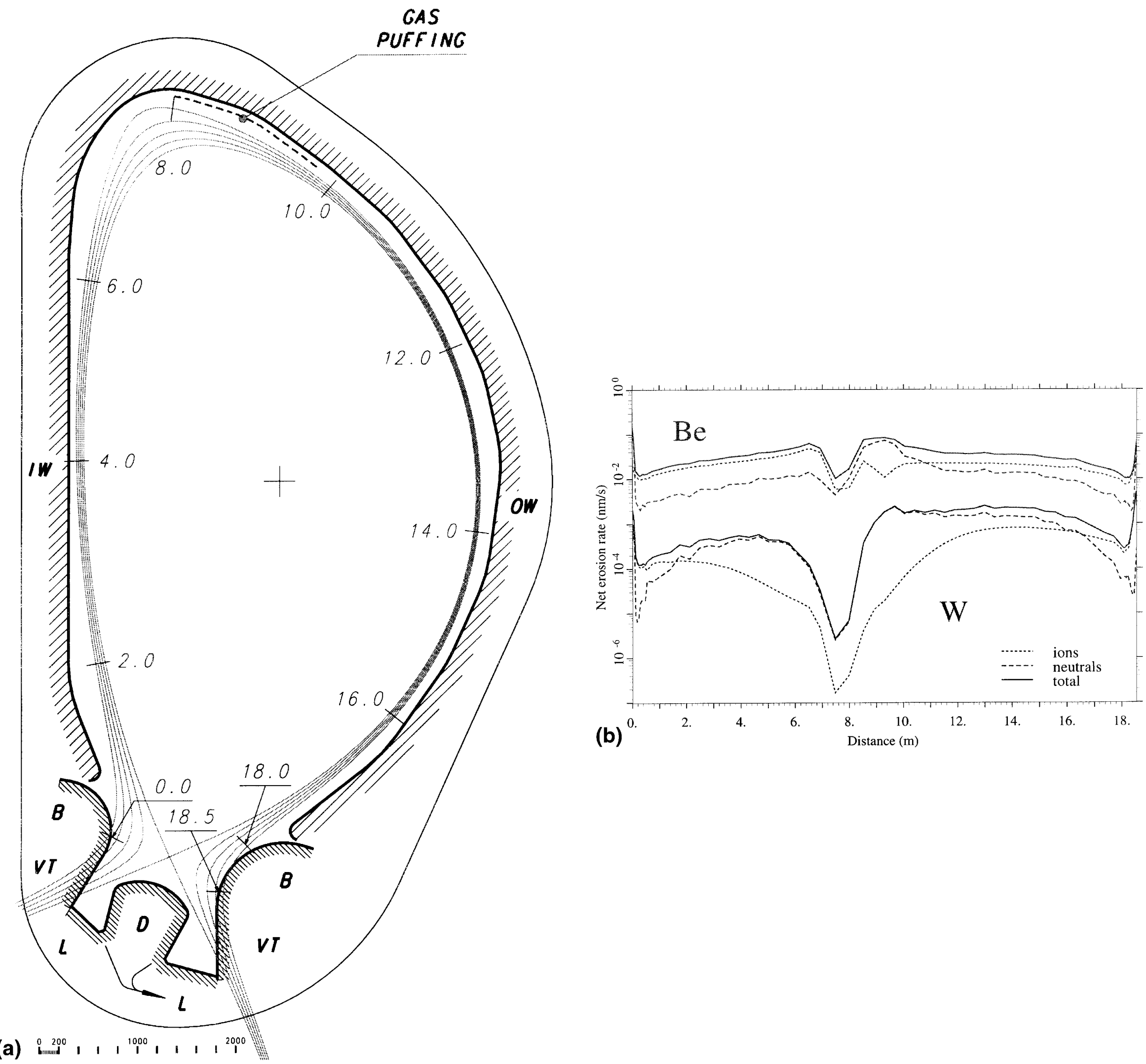

Fig. 4. (a) ITER-FEAT poloidal cross-section showing vacuum vessel (inner contour), divertor vertical target (VT), divertor baffle (B), and divertor private region consisting of dome (D) liner (L), and inner (IW) and outer (OW) first-wall. Start-up limiters (2 modules) are located at the equatorial level. SOL magnetic surfaces including separatrix are shown (the outermost surface limits the EIRENE calculation grid, numbers are distance in metres along this line). (b) Erosion rate on the main chamber wall for Be and W plotted along the EIRENE calculation grid as described in Fig. 4(a). The $\sim$ factor 10 lower erosion rate for W as well as the large reduction of the erosion rate near the gas inlet (lower average temperature of the neutrals) for both materials can be seen.

gible, making W the preferred divertor PFM for a reactor.

The impact of abnormal events such as disruptions on the lifetime of CFC and W clad divertor HHF components has also to be included. During disruptions, energy loads of up to 30 MJ m^{-2} are deposited on the divertor strike zone area and vapor shields develop, which are optically thick, stopping the incoming plasma and transferring its energy into radiation. As a result the whole of each V-shaped divertor leg is filled with a radiation field which causes secondary vapor shields to occur and thus transfers a more or less equal amount of energy to all surfaces in the divertor [43]. Therefore vaporization and melting (in case of W) will occur on all divertor surfaces. When comparing the amount of material lost during such an event it is in the order of several μm in the case of CFC clad targets and in the order of 80 μm in the case of W clad targets [43]. The resulting disruption lifetime for 2 cm CFC is very large while for 1 cm W it is in the order of 100 disruptions if the whole melt layer is lost during the energy deposition and if the strike zone would be always at the same position. Most of the melt layer (80%) is just shifted sideways and thus moderate relocation of the strike zones which will happen naturally might significantly increase this number.

3.2. T-co-deposition

Besides the erosion lifetime the amount of T trapped per discharge is of great importance and will strongly influence the PFM choice in ITER. Analysis [36] yields 0.1 to 0.4 g T per 400 s discharge trapped due to co-deposition with Be eroded from the FW and 1 g to 2 g T per 400 s discharge trapped due to co-deposition with C (includes chemical sputtering). While the 0.1–0.4 g T-co-deposited with Be is a rather conservative value (is most likely lower) because it is based on high trapping rates measured in laboratory plasmas with large oxygen contamination, the $\sim$1–2 g T per discharge trapped by co-deposition with C seems to be realistic. Considering also a safety limit for the total amount of T to be trapped inside the ITER vessel of 450–1000 g (site dependent) only 180–350 discharges will be possible before a cleaning process must be started. However, to date no reliable and fast cleaning method is known [6,10]. In addition, results reported in [49] suggest that co-deposition of T with C can take place a long distance away from the plasma strike zones due to the formation of hydro carbon molecules with very low sticking coefficients. If the predictions for T-co-deposition with C remain as stated above and no efficient in situ cleaning method can be found, it is unlikely that CFC can be used as a PFM in a D–T machine like ITER.

3.3. Dust production

A further issue is the problem of dust production. The definition of dust is somewhat uncertain but particle sizes <100 μm can be considered as dust. However, most safety hazards discussed below originate from much smaller particle sizes ($\ll 10$ μm) which have in fact been found in existing experiments, albeit in small amounts, while larger particle sizes (>100 μm such as C-flakes) dominate the total mass of dust. Small size dust particles can cause in principle two main safety hazards in a nuclear machine like ITER if certain quantities are exceeded namely, either a breach of the confinement (in safety terms) due to an explosion caused directly or indirectly by dust, or a contamination of the buildings and ultimately of the environment if highly radioactive dust is blown out of the vessel during a sudden major air in-break (break of large diagnostic/heating system windows).

In the case of Be, the main concern is its chemical exothermal and thus self sustained reaction with steam (water leak) if the surface temperature exceeds $\sim$350°C which leads to the production of hydrogen. While most of the plasma facing components will remain below this temperature even if a loss of coolant accident (LOCA) occurs, Be dust located on W surfaces, which are subject to high disruption or VDE loads, might exceed the critical temperature. Because of the large surface area of small dust particles ($\ll 10$ μm) they are chemically highly active resulting in a safety limit of <20 kg of Be dust on potentially hot surfaces such as the W clad divertor dome. Since this limit is a safety limit aimed at keeping the amount of produced hydrogen below the explosion limit, a permanent safety licensed monitoring of Be dust on critical surfaces or a very convincing argument why the amount of dust will always be below this limit will be needed in order to get permission to operate ITER. In case of the divertor dome a possible argument is that Be dust will only accumulate in the groves between the W tiles and that this volume is too small to hold 20 kg. In addition to the limit for potentially hot surfaces a general limit of 100 kg Be dust inside the ITER vessel exists. Again, a certified monitoring system will need to be developed which is a subject for future work.

In case of C dust a limit of $\sim$100 kg inside the ITER vessel exists which is related to a potential carbon dust explosion as sometimes observed in coal mines. In the latter case it is assumed that an air in break occurs which mobilizes all the C dust and thus provides an explosive mixture. Again a method to monitor the amount of C dust will have to be developed.

In the case of highly activated W dust the issue is the possible contamination of the environment resulting from an air in break which mobilizes the dust. As the limit for W dust is not related to an explosion limit the allowed amount will only depend on the ability of the ITER building to stop contamination from spreading into the environment and on the site specific release limits. Therefore $\sim$100–300 kg of W dust will be allowed in the ITER vessel. Due to the potential safety hazard the burden of proof that dust limits are not exceeded is on the side of the ITER design team. Therefore, it is of utmost importance to understand the mechanisms of dust production for each of the envisaged PFMs, the dependence on their location (e.g., FW, divertor, etc), the size distribution of the produced dust particles and to develop monitoring as well as cleaning systems with minimum impact on the machine operation schedule.

Several possible mechanisms for dust production have been identified but a quantification of the importance of each of them remains largely unclear. The best understood production mechanism is the flaking of redeposited material which is practically only observed for layers of co-deposited C and hydrogen. This mechanism is the main source of the larger dust particles which form by far the majority of dust in terms of weight in existing machines. Ideas about the production mechanism of smaller particle sizes and thus of the metallic dust found in present devices are so far only qualitative.

- Small dust particles ($\ll 10$ μm) could condense in cold plasma or gas from sputtered or more likely from evaporated material during large ELMs or disruptions [50].
- Evaporation by arcing during plasma operation [51] and a following condensation before the material is redeposited on a surface has also been suggested.

Very rough preliminary estimates were made to determine the amount of dust produced per discharge in ITER it was assumed that a fraction of the evaporated material (50%) during disruptions ends up as dust as well as 10% of the sputtered material. The result of this crude and uncertain estimate assuming 10% of the discharges end in disruptions and 1% in VDEs yield that the dust limits will be reached in a time comparable to – or larger than the lifetime of the divertor components, i.e., they will most likely not impact the operation schedule. However, the error bars of these estimates are very large and will not improve before a better understanding of dust production mechanisms is developed on existing machines.

4. Plasma facing materials choice

The above discussed plasma–wall interaction behavior of the envisaged PFMs need all be taken into account in the choice of the plasma facing material for the different areas in the ITER machine (Fig. 4(a)). The ability to give more weight to the plasma–wall interaction issues when making a PFM choice is possible because during the past 6 years of the ITER-EDA progress in design supported by R&D has shown that CFC and W can be used with equal confidence as cladding material for the divertor targets from the engineering point of view, and several solutions exist for Be as FW material in the main plasma chamber [44,52–55].

The choice of Be as the FW material in the main chamber of ITER is rather straight forward due to the larger number of VDEs it can withstand when compared to W. An additional advantage is its low Z and the proven ability to provide clean plasmas (e.g., oxygen gettering) as long as the heat loads are such that no evaporation occurs. However, Be will only be acceptable for a low duty cycle machine such as ITER and not for a reactor where high Z materials like W appear to be the only choice. In addition the above mentioned safety issues with dust might in the future cause a strong pressure to move towards a single PFM machine where no dust related explosion limits exist. This should provide a strong incentive for present day machines to consider the use of high Z (Mo, W) as their main chamber wall material in order to have a broader experimental basis for such a decision should it be necessary.

The choice of material becomes more difficult in the divertor area due to the wide range of issues, i.e., from T-co-deposition (CFC) to disruption erosion and melting (W) as well as possible mixed material effects. In the 1998 ITER design and up to now also in the new ITER design the reference divertor PFMs are W for the dome and the liner as well as for the less loaded upper part of the vertical targets and a small area $\sim$50 m^2 of CFC cladding at the highest loaded strike zones. The rationale for this choice is that CFC will neither heavily erode during disruptions nor melt. In addition during the initial operation phase where a higher disruption frequency is expected the disruption lifetime of W might be marginal due to melt layer losses. In the rest of the divertor W is acceptable because these areas are receiving high CX fluxes and W will erode very little. The melting during disruptions is probably also acceptable there because the electromagnetic forces pushing the melt layer sideways on the strike zone will most likely be smaller.

This rationale has been based on the assumption that the tritium co-deposition problem can be solved by, e.g., operating the divertor target surfaces at higher temperatures [52]. However, the results reported in [49] and the results from existing tokamaks as well as from modeling [10,36,42] suggest that several gram of T could be trapped in each ITER discharge while no proven cleaning method exists to date. Therefore, it is considered to clad the whole divertor with W at least before deuterium and tritium are introduced in the machine, i.e., after the 2 year long Hydrogen phase where human access is possible.

In addition to replacing the divertor targets, it will be necessary to thoroughly clean the carbon from all in-vessel surfaces, since the residual layers will continue to have the potential to collect T by isotope exchange. Hence, even if carbon is considered only for the H phase, methods need to be developed that can adequately remove the carbon deposits. Apart from mechanical methods, baking in the presence of a partial pressure of oxygen has been shown to be effective in removing the soft hydrogenated carbon layers responsible for retaining most of the tritium. The bake, at a temperature of >250°C (possibly >350°C), may take many days or even weeks to be effective, but could be worthwhile as a one-off event prior to a switch to an all tungsten armour.

5. Summary and conclusions

As in 1998 the ITER parties were unable to provide the necessary funds for the construction of the ITER design it was decided to develop a smaller size ITER with reduced performance objectives and a goal to reduce the cost by 50%. After studying several possible options with a major radius of $\sim$6.2 m it was concluded that the best compromise between the different physics goals and the cost is achieved in an intermediate aspect ratio machine (3.1).

While the general layout and design of the machine as well as its performance capability is quite satisfactory, some issues, concerning among other things plasma–wall interaction, remain to be solved either by improved physics knowledge to be generated by the existing worldwide fusion program or by changes of details in the design. The most important issue in this category is the only marginal compatibility of the divertor target melt and vaporization limits with the expected ELM energy load during Type-I ELMy H-mode operation, i.e., the reference regime. Here research in existing machines has to focus on reducing the ELM size without degrading confinement and/or substantiating existing back-up regimes such as Type-II ELMy H-mode or RI-mode as well as density profile peaking by pellet injection. This is even more important because no significant mitigation of this problem can be expected from design variations.

In case of the second main operation mode, namely the steady-state operation with ITB, it might be possible to cope with the expected high divertor heat loads partially by a change of the divertor geometry and by changing the plasma facing material. However, the problem of fatigue lifetime of the heat sink might persist at peak power loads significantly exceeding 10 MW m^{-2}, which will limit the total number of this kind of pulses to <1000. As the prediction of the behavior of ITB discharges in ITER–FEAT is much less certain than for inductive operation, and as progress in this area in existing machines is large, also improved physics knowledge might help to mitigate this problem in the future.

When considering the erosion lifetimes of the different plasma facing components in their reference configuration (Be-FW, CFC strike zone, W cladding on all other divertor components) one can certainly say that they are adequate for a low duty cycle experimental machine like ITER. Issues such as T retention due to codeposition as well as dust production might finally force the use of a single material, i.e. W, even in ITER. Therefore the application of W as PFM in existing machines and thus the enhancement of the experience in operation with high Z walls is a very important task.

Finally, one can say that regardless of some remaining problems or in some cases small margins, ITER has a comfortable balance of experimental risk and confidence to achieve its goals. If it is built one can be certain that it will be possible to solve remaining problems which are already recognized due to the experimental flexibility and sound design of ITER.

Acknowledgements

I would like to acknowledge the contributions of G. Federici and H. Wuerz who supported me with fruitful discussions and a lot of data. This report has been prepared as an account of work performed under the Agreement among the European Atomic Energy Community, the Government of Japan, and the Government of the Russian Federation on Co-operation in the Engineering Design Activities for the International Thermonuclear Experimental Reactor ("ITER EDA Agreement") under the auspices of the International Atomic Energy Agency (IAEA).

References

[1] INTOR, Phase Two A, Part III, IAEA, Vienna, 1988.
[2] ITER CDA Final Report, IAEA, Vienna, 1991.
[3] R. Aymar, V. Chuyanov, M. Huguet et al., in: Proceedings of 16th IAEA Fusion Energy Conference, vol. 1, Montreal, Canada, 1997, p. 3.
[4] Y. Seki, M. Kikuchi, T. Ando et al., in: Proceedings of the 13th IAEA Conference on Plasma Physics Controlled Fusion, Washington, DC, IAEA-CN-53/G-1-2, 1990.
[5] Technical Basis for the ITER Final Design Report, Cost Review and Safety Analysis, (FDR) ITER EDA Documentation Series No. 16, IAEA, Vienna, 1998.
[6] G. Federici et al., J. Nucl. Mater. 266–269 (1999) 14.
[7] G. Janeschitz et al., J. Nucl. Mater. 220–222 (1995) 73.
[8] A. Leonard et al., J. Nucl. Mater. 266–269 (1999) 109.
[9] Horst Pacher, I. Smid, G. Federici et al., J. Nucl. Mater. 241–243 (1997) 255.
[10] G. Federici et al., Issues arising from plasma material interactions in reactor class tokamaks, review paper, Nucl. Fus., to be published.
[11] G. Janeschitz et al., Nucl. Fus. 4 (6) (2000) 1197.
[12] ITER Special Working Group report, 1999.
[13] F.X. Söldner, Plasma Phys. Control. Fus. 39 (1997) B353.
[14] T. Fujita, S. Ide, H. Shirai et al., Phys. Rev. Lett. 78 (1997) 2377.
[15] R.C. Wolf et al., in: Proceedings of the 17th IAEA Fusion Energy Conference, Yokohama, Japan, IAEA-F1-CN-69/EXP1/12, 1998.
[16] E.A. Lazarus, G.A. Navratil, C.M. Greenfield et al., Nucl. Fus. 37 (1997) 7.
[17] E.J. Synakowski et al., Phys. Plasmas 4 (1997) 1736.
[18] ITER-FEAT Outline Design Report, ITER EDA Documentation Series, IAEA, Vienna, 2000, to be published.
[19] ITER Physics Basis, Nucl. Fus. 39 (1999) 2137.
[20] G. Saibene, L.D. Horton, R. Sartori et al., Nucl. Fus. 39 (1999) 1133.
[21] J. Stober et al., in: Proceedings of the 26th EPS Conference on Controlled Fusion and Plasma Physics, ECA, 23J, Maastricht, 1999, p. 1401.
[22] O. Gruber et al., in: Proceedings of the 17th IAEA Fusion Energy Conference, Yokohama, Japan, IAEA-F1-CN-69/OV4/3, 1998.
[23] Y. Kamada et al., in: Proceedings of the 17th IAEA Fusion Energy Conference, Yokohama, Japan, IAEA-F1-CN-69/CD2/EX9/2, 1998.
[24] G. Janeschitz, Yu. Igitkhanov, M. Sugihara et al., in: Proceedings of the 26th the EPS Conference on Controlled Fusion Plasma Physics, Maastricht, 1999, p. 1445.

[25] M. Sugihara, Y. Igitkhanov, G. Janeschitz, Nucl. Fus. 40 (10) (2000) 1743.
[26] G. Janeschitz et al., in: Proceedings of the Fifth International Symposium on Fusion Technology, Rome, 1999, Fusion Eng. Des., to be published.
[27] A. Kukushkin et al., in: Proceedings of the 26th the EPS Conference on Controlled Fusion Plasma Physics, Maastricht, 1999, p. 1545.
[28] A. Kukushkin et al., these Proceedings.
[29] V. Mukhovatov et al., in: Proceedings of the Seventh IAEA TCM on H-mode and Transport Barrier Physics, Oxford, September 1999.
[30] M. Kotchenreuter et al., in: Proceedings of the 16th IAEA Fusion Energy Conference, IAEA-F1-CN-64/D1-5, Montreal, Canada, 1996.
[31] M. Sugihara, Y. Igitkhanov, G. Janeschitz et al., in: Proceedings of the 26th the EPS Conference on Controlled Fusion Plasma Physics, Maastricht, 1999, p. 1449.
[32] J. Stober et al., in: Proceedings of the Seventh IAEA Workshop on H-mode physics and Transport Barriers, Oxford, 1999, to be published in PPCF.
[33] A. Leonard et al., J. Nucl. Mater. 266–269 (1999) 109.
[34] G.M. Fishpool, Nucl. Fus. 38 (1998) 1373.
[35] A. Leonard et al., these Proceedings.
[36] G. Federici et al., Assessment of Erosion and co-deposition in ITER-FEAT, these Proceedings.
[37] Y. Kamada et al., in; Proceedings of the Seventh IAEA TCM on H-mode and Transport Barrier Physics, Oxford, September 1999.
[38] T. Ozeki et al., Nucl. Fus. 30 (1990) 1425.
[39] M. Greenwald et al., in: Proceedings of the 17th IAEA Fusion Energy Conference, IAEA-F1-CN-69/EX1/4, Yokohama, 1998.
[40] V.P. Bahtnagar et al., in: Proceedings of the 18th EPS Conference on Controlled Fusion and Plasma Physics, vol. 1, 1991, p. 369.
[41] A. Messian et al., Phys. Rev. Lett. 77 (1996) 2487.
[42] A. Sakasai et al., in: Proceedings of the 17th IAEA Fusion Energy Conference, IAEA-F1-CN-69/EX6/5, Yokohama, 1998.
[43] H. Würz et al., these Proceedings.
[44] V. Barabash et al., in: Proceedings of the 20th Symposium on Fusion Technology, vol. 1, Marseille, France, 7–11 September 1998, pp. 215–218.
[45] A. Cardella et al., J. Nucl. Mater. 283–287 (2000) 1105.
[46] A.R. Rafray et al., in: B. Beaumont et al.,(Eds.), Proceedings of 20th Symposium on Fusion Technology, vol. 1, Marseille, France, 1998, p. 211.
[47] G. Pautasso et al., these Proceedings.
[48] J.N. Brooks, Nucl. Technol. Fus. 4 (1983) 33.
[49] A. von Keudell, C. Hopf, T. Schwarz-Selinger, W. Jacob, Nucl. Fusion 37 (1999) 1451.
[50] J. Winter, G. Gebauser, J. Nucl. Mater. 266–269 (1999) 228.
[51] R. Behrisch, Surface erosion by electrical arcs, in: D.E. Post, R. Behrisch, (Eds.), Physics of Plasma–Wall Interactions in Controlled Fusion (NATO ASI Series B: Physics) Plenum Press, New York, 1986, p. 495.
[52] C. Ibbott et al., in: Proceedings of ISFNT-5, Rome, 1999, Fus. Eng Des., to be published.
[53] G. Vieider et al., European development of prototypes for ITER high heat flux components, in: Proceedings of ISFNT-5, Rome, 1999, Fus. Eng. Des., to be published.
[54] P. Chappuis et al., IAEA Technical Meeting on SSO of MFD 1999, Nucl. Fus., to be published.
[55] K. Ioki et al., J. Nucl. Mater. 283–287 (2000) 957.